Lossless Convexification of Control Constraints for a Class of Nonlinear Optimal Control Problems

Lars Blackmore, Behçet Açıkmeşe and John M. Carson III

***Abstract*— In this paper we consider a class of optimal control problems that have continuous-time nonlinear dynamics and nonconvex control constraints. We propose a convex relaxation of the nonconvex control constraints, and prove that the optimal solution to the relaxed problem is the globally optimal solution to the original problem with nonconvex control constraints. This lossless convexification enables a computationally simpler problem to be solved instead of the original problem. We demonstrate the approach in simulation with a planetary soft landing problem involving a nonlinear gravity field.**

I. Introduction

In this paper we consider a class of finite time horizon optimal control problems that have continuous-time nonlinear dynamics and nonconvex control constraints. A large number of practical problems fall into this category. One example is the planetary landing problem[13], [12], also known as the soft landing problem in the optimal control literature[9]. In planetary landing, an autonomous spacecraft lands on the surface of a planet by using thrusters, which can produce a finite magnitude force vector with an upper and nonzero lower bound on the magnitude. In this case, the resulting set of feasible controls is nonconvex. Another example is that of path planning for an unmanned aerial vehicle (UAV) subject to upper and lower bounds on the norm of the commanded velocity[15]. As with the soft landing problem, the minimum norm constraint makes the set of feasible controls nonconvex.

Prior work proposed the idea of relaxing the nonconvex control constraints to a convex set in such a way that the optimal solution to the relaxed problem is guaranteed to be the optimal solution to the original problem[2]. We refer to this as a lossless convexification, since no part of the feasible space of the original problem is removed in the process of rendering the constraints convex. In [2], [5] the authors perform a lossless convexification for the special case of a planetary landing problem in a constant gravity field, where the changing mass of the spacecraft renders the system dynamics nonlinear. In [1] this result is generalized to optimal control problems with linear system dynamics and a class of non-convex control constraints. In the present paper we establish an extension of this result to a class of optimal control problems with nonlinear system dynamics and nonconvex control constraints. This class includes the planetary landing problem with nonlinear, nonconstant gravity fields and aerodynamic forces. The extension to nonconstant gravity fields is significant, since it extends the applicability of convexification from landing on large planets, where gravity may be assumed constant, to small bodies such as moons, comets and asteroids. General nonlinear dynamics prevent the finite-parameter optimization problem that results from the convexification from being convex; however by approximating the nonlinear dynamics as being piecewise linear, the **globally** optimal solution can be found in finite time using Mixed Integer Linear Programming (MILP)[10]. This is in contrast to shooting or pseudospectral methods[8], [18], [16], which can only guarantee **local** optimality. By removing the nonconvex control constraints, the convexification introduced in this paper significantly reduces the number of disjunctions in the MILP encoding, and hence the problem complexity.

The organization of the paper is as follows. In Section II we provide the main theoretical result, in Section III we show how the result applies to two practical examples, and in Section IV we provide simulation results.

II. Lossless Convexification

In this section we provide our main analytic result, namely lossless convexification for a class of nonlinear optimal control problems with nonconvex control constraints. We provide a convex relaxation of the nonconvex control constraints, along with guarantees that the optimal solution to the problem with the convex control constraints is the optimal solution to the problem with nonconvex control constraints.

In this paper we consider the nonlinear dynamic system:

$$\dot{\mathbf{x}} = \mathbf{f}\big(t, \mathbf{x}, \mathbf{u}, g_c(\mathbf{u})\big), \tag{1}$$

where $\mathbf{x} \in \Re^{n_x}$, the function $\mathbf{f}$ is continuously differentiable, and $g_c : \Re^{n_u} \to \Re^1$ is a measure of the control effort. We use $\mathbf{u} \in \Re^{n_u}$ to denote the control inputs. We use $||\mathbf{v}||$ to denote the 2-norm of vector $\mathbf{v}$. We use $\mathbf{v} = 0$ to mean that all elements of $\mathbf{v}$ are zero, and use $\mathbf{v} \neq 0$ to mean that at least one element of $\mathbf{v}$ is nonzero. A vector of all zeros except unity in the i'th element is denoted $\mathbf{e}_i$. We use a.e. to mean 'almost everywhere', i.e. everywhere except on a set of measure zero. We define the Jacobian of an arbitrary

This research was carried out at the Jet Propulsion Laboratory (JPL), California Institute of Technology, under a contract with the National Aeronautics and Space Administration. Government sponsorship acknowledged.

L. Blackmore (corresponding author) is a Senior GNC Engineer, Space Exploration Technologies. lars.blackmore@spacex.com

B. Açıkmeşe is a Technologist, JPL, California Institute of Technology. behcet@jpl.nasa.gov

J. Carson is a Guidance and Control Engineer, JPL, California Institute of Technology. jmcarson@jpl.nasa.gov

function $\mathbf{h}(\mathbf{v}) : \Re^{n_v} \rightarrow \Re^{n_h}$ as follows:

$$(\nabla_{\mathbf{v}}\mathbf{h}) \triangleq \begin{bmatrix} \frac{\partial h_1}{v_1} & & \frac{\partial h_{n_h}}{v_1} \\ & \ddots & \\ \frac{\partial h_1}{v_{n_v}} & & \frac{\partial h_{n_h}}{v_{n_v}} \end{bmatrix},$$

where h_i denotes the i'th element of $\mathbf{h}$ and v_i denotes the i'th element of $\mathbf{v}$.

In this paper we are concerned with the optimal control problem:

Problem 1 (With non-convex control constraints):

$$\min_{\mathbf{u},t_f} J = \int_0^{t_f} l\big(t, g_c(\mathbf{u}(t))\big)dt \qquad \text{subject to:} \tag{2}$$

$$\dot{\mathbf{x}}(t) = \mathbf{f}(t, \mathbf{x}(t), \mathbf{u}(t), g_c(\mathbf{u}(t))) \quad \text{a.e. on } [0, t_f] \tag{3}$$

$$0 < \rho_1 \leq g_c(\mathbf{u}(t)) \leq \rho_2 \quad \text{a.e. on } [0, t_f] \tag{4}$$

$$\mathbf{x}(0) = \mathbf{x}_0, \quad \mathbf{x}(t_f) \in \mathcal{F}. \tag{5}$$

We propose the following **convex** relaxation of the control constraints in Problem 1, which is inspired by the convexification introduced in [2], [5], [1]:

Problem 2 (With relaxed control constraints):

$$\min_{\mathbf{u},t_f,\Gamma} J = \int_0^{t_f} l\big(t, \Gamma(t)\big)dt \qquad \text{subject to:} \tag{6}$$

$$\dot{\mathbf{x}}(t) = \mathbf{f}(t, \mathbf{x}(t), \mathbf{u}(t), \Gamma(t)) \quad \text{a.e. on } [0, t_f] \tag{7}$$

$$0 < \rho_1 \leq \Gamma(t) \leq \rho_2 \quad \text{a.e. on } [0, t_f] \tag{8}$$

$$g_c(\mathbf{u}(t)) \leq \Gamma(t) \qquad \text{a.e. on } [0, t_f] \tag{9}$$

$$\mathbf{x}(0) = \mathbf{x}_0, \quad \mathbf{x}(t_f) \in \mathcal{F}, \tag{10}$$

where $\Gamma(t) \in \Re^1$ is a slack variable.

The following lemma establishes conditions under which the optimal value of $\mathbf{u}$ is on the boundary of the feasible set.

Lemma 1: Let:

$$H = \lambda_0 l(t, \Gamma) + \lambda^T \mathbf{f}(t, \mathbf{x}, \mathbf{u}, \Gamma).$$

Let:

$$\{\mathbf{u}^\dagger, \Gamma^\dagger\} \triangleq \arg\max_{\mathbf{u},\Gamma} H$$
$$\text{subject to } \; g_c(\mathbf{u}) \leq \Gamma,\, 0 < \rho_1 \leq \Gamma \leq \rho_2.$$

Then if $\mathbf{f}(t, \mathbf{x}, \mathbf{u}, \Gamma)$ is differentiable in $\mathbf{u}$ and $(\nabla_{\mathbf{u}}\mathbf{f})\lambda \neq 0$ at $\mathbf{u}^\dagger$:

$$g_c(\mathbf{u}^\dagger) = \Gamma^\dagger.$$

Proof: The pair $\{\mathbf{u}^\dagger, \Gamma^\dagger\}$ must satisfy:

$$\mathbf{u}^\dagger = \arg\max_{\mathbf{u}} \lambda^T \mathbf{f}(t, \mathbf{x}, \mathbf{u}, \Gamma^\dagger) \quad \text{subject to:} \tag{11}$$

$$g_c(\mathbf{u}) \leq \Gamma^\dagger. \tag{12}$$

If at $\mathbf{u}^\dagger$, $\partial H/\partial \mathbf{u} = (\nabla_{\mathbf{u}}\mathbf{f})\lambda \neq 0$ then gradient of the cost function (11) is nonzero at $\mathbf{u}^\dagger$. Hence the optimal solution to (11) is on the boundary of the feasible set, and $g_c(\mathbf{u}^\dagger) = \Gamma^\dagger$. ■

Condition 1: The pair $[-(\nabla_{\mathbf{x}}\mathbf{f}), (\nabla_{\mathbf{u}}\mathbf{f})]$ is totally observable[7] on $[0, t_f]$ for all sequences of $\mathbf{x}$ and $\mathbf{u}$ satisfying (7) through (10), meaning that for every subinterval $[t_1, t_2] \subseteq [0, t_f^*]$ the initial state $\lambda(t_1)$ of the following system can be determined uniquely from the output $\mathbf{y}(t)$ for $t \in [t_1, t_2]$:

$$\dot{\lambda} = -(\nabla_{\mathbf{x}}\mathbf{f})\lambda$$
$$\mathbf{y} = (\nabla_{\mathbf{u}}\mathbf{f})\lambda. \tag{13}$$

The following theorem provides the lossless convexification that is the main result of this paper.

Theorem 1: Let $\{\mathbf{u}^*, \mathbf{x}^*, t_f^*, \Gamma^*\}$ be the optimal solution to Problem 2. If Condition 1 is satisfied, the function $l(t, \Gamma) \neq 0 \quad \forall \Gamma \in [\rho_1, \rho_2],\ \forall t$, then $\{\mathbf{u}^*, \mathbf{x}^*, t_f^*\}$ is the optimal solution to Problem 1.

Proof: The Hamiltonian for Problem 2 is:

$$H = \lambda_0 l(t, \Gamma) + \lambda^T \mathbf{f}(t, \mathbf{x}, \mathbf{u}, \Gamma), \tag{14}$$

and the costate dynamics are given by:

$$\begin{bmatrix} \dot{\lambda}_0 \\ \dot{\lambda} \end{bmatrix} = -\frac{\partial H}{\partial \mathbf{x}} = \begin{bmatrix} 0 \\ -(\nabla_{\mathbf{x}}\mathbf{f})\lambda \end{bmatrix}, \tag{15}$$

where λ_0 is constant and λ is absolutely continuous with $[\lambda_0, \lambda^T] \neq 0\ \forall t$ from [3]. Define $\mathbf{y} = (\nabla_{\mathbf{u}}\mathbf{f})\lambda$. We now show that $\mathbf{y}(t) = 0$ for a finite interval is not possible. The proof is by contradiction. Assume that there exists $t_1 < t_2$ such that $\mathbf{y}(t) = 0 \quad \forall t \in [t_1, t_2]$. From Condition 1 the system (13) is totally observable on the interval $[0, t_f^*]$, meaning that for every subinterval $[t_1, t_2] \subseteq [0, t_f^*]$ the initial state $\lambda(t_1)$ can be determined uniquely from the output $\mathbf{y}(t)$ for $t \in [t_1, t_2]$. This means that $\lambda(t_1) = 0$, and from the costate dynamics $\lambda(t) = 0 \quad \forall t \in [t_1, t_f^*]$. Since t_f is unconstrained, the transversality condition[3] means that $H(t_f^*) = 0$, and since $l(t, \Gamma) \neq 0 \quad \forall t, \forall \Gamma \in [\rho_1, \rho_2]$ this means that $\lambda_0 = 0$, hence $[\lambda_0, \quad \lambda^T] = 0 \quad \forall t \in [t_1, t_f^*]$, which contradicts the requirement that $[\lambda_0, \quad \lambda^T]^T \neq 0 \quad \forall t \in [0, t_f^*]$. Hence $\mathbf{y}(t) \neq 0$ a.e on $t \in [0, t_f^*]$.

The pointwise maximum principle implies that, in the optimal solution, the Hamiltonian is maximized over $\{\mathbf{u}, \Gamma\}$ almost everywhere on $t \in [0, t_f^*]$. For any value of Γ, since $(\nabla_{\mathbf{u}}\mathbf{f})\lambda \neq 0$ a.e. on $t \in [0, t_f^*]$, Lemma 1 means that $g_c(\mathbf{u}^*) = \Gamma$ a.e. on $t \in [0, t_f^*]$. Hence the cost functions (2) and (6) for the nonconvex problem and the relaxed problem are identical, and the nonconvex control constraint (4) is satisfied by $\mathbf{u}^*$. Furthermore the relaxed solution satisfies the original dynamics (3). This implies that the optimal cost of Problem 2 is greater than or equal to the optimal cost of Problem 1. Since Problem 2 is a relaxation of Problem 1, the optimal cost of Problem 2 is less than or equal to the optimal cost of Problem 1. Hence the costs are equal, which completes the proof. ■

Theorem 1 shows that we can solve a relaxation (Problem 2) of the nonconvex optimal control problem (Problem 1) with a guarantee that the optimal solution to the relaxation will be the globally optimal solution to the original problem. We have hence established a lossless convexification of Problem 1.

Condition 1 can be established using the following result from [7]:

Lemma 2: The system (13) is totally observable on the interval $[0, t_f]$ if and only if the following *observability matrix* has rank n_x almost everywhere on $[0, t_f]$:

$$Q(t) \triangleq [(\nabla_{\mathbf{u}}\mathbf{f})^T, \Delta_0(\nabla_{\mathbf{u}}\mathbf{f})^T, \ldots, \Delta_0^{n-1}(\nabla_{\mathbf{u}}\mathbf{f})^T]^T, \quad (16)$$

where:

$$\Delta_0 \equiv (\nabla_{\mathbf{x}}\mathbf{f})^T + \frac{d}{dt}, \quad (17)$$

and $(\nabla_{\mathbf{x}}\mathbf{f})$ and $(\nabla_{\mathbf{u}}\mathbf{f})$ are $n_x - 2$ and $n_x - 1$ times differentiable, respectively.

The rank of the matrix $Q(t)$ may be difficult to verify, in general, because of the need to compute the time-derivatives in (17). For a large class of problems related to vehicle path planning, we can show that Condition 1 is satisfied without the need for explicit computation of the derivatives. In such problems the state can be partitioned into two parts; the first is acted upon directly by the control effort, the second is not. An example is where the control effort acts to change the vehicle velocity, and the vehicle's position is simply the integral of velocity. The following corollary shows that for such systems, the convexification holds:

Corollary 1: Let $\{\mathbf{u}^*, \mathbf{x}^*, t_f^*, \Gamma^*\}$ be the solution to Problem 2 where $f(\cdot)$ has the form:

$$\mathbf{x} = \begin{bmatrix}\mathbf{x}_1\\ \mathbf{x}_2\end{bmatrix} \qquad f(t, \mathbf{x}, \mathbf{u}) = \begin{bmatrix}\mathbf{f}_1(t, \mathbf{x}, \mathbf{u})\\ \mathbf{f}_2(t, \mathbf{x})\end{bmatrix}. \quad (18)$$

If $\text{Null}(\nabla_{\mathbf{u}} f_1) = 0$, $\text{Null}(\nabla_{\mathbf{x}_1} f_2) = 0$, the function $l(t, \Gamma) \neq 0 \;\; \forall \Gamma \in [\rho_1, \rho_2], \; \forall t$, then $\{\mathbf{u}^*, \mathbf{x}^*, t_f^*\}$ is the optimal solution to Problem 1.

Proof: For this system:

$$\begin{aligned}(\nabla_{\mathbf{u}}\mathbf{f}) &= \begin{bmatrix}(\nabla_{\mathbf{u}}\mathbf{f}_1) & 0\end{bmatrix}\\ (\nabla_{\mathbf{x}}\mathbf{f}) &= \begin{bmatrix}(\nabla_{\mathbf{x}_1}\mathbf{f}_1) & (\nabla_{\mathbf{x}_1}\mathbf{f}_2)\\ (\nabla_{\mathbf{x}_2}\mathbf{f}_1) & (\nabla_{\mathbf{x}_2}\mathbf{f}_2)\end{bmatrix}\end{aligned} \quad (19)$$

Define:

$$M(t) \triangleq [(\nabla_{\mathbf{u}}\mathbf{f})^T, \Delta_0(\nabla_{\mathbf{u}}\mathbf{f})^T]^T, \quad (20)$$

then:

$$M(t) = \begin{bmatrix}(\nabla_{\mathbf{u}}\mathbf{f}_1) & 0\\ \frac{d(\nabla_{\mathbf{u}}\mathbf{f}_1)}{dt} - (\nabla_{\mathbf{u}}\mathbf{f}_1)(\nabla_{\mathbf{x}_1}\mathbf{f}_1) & -(\nabla_{\mathbf{u}}\mathbf{f}_1)(\nabla_{\mathbf{x}_1}\mathbf{f}_2)\end{bmatrix} \quad (21)$$

We now show that $M(t)$ has rank n_x. It suffices to show that $M(t)\lambda = 0$ implies $\lambda = 0$. Let $\lambda = (\lambda_1, \lambda_2)$, then $\text{Null}(\nabla_{\mathbf{u}}\mathbf{f}_1) = 0$ implies $\lambda_1 = 0$, hence $(\nabla_{\mathbf{u}}\mathbf{f}_1)(\nabla_{\mathbf{x}_1}\mathbf{f}_2)\lambda_2 = 0$. Since $\text{Null}(\nabla_{\mathbf{x}_1}\mathbf{f}_2) = 0$, this implies $\lambda_2 = 0$ and hence $\lambda = 0$, and Null($M(t)$)=0. Hence, for the system (18), $Q(t)$ is rank n_x and the conditions of Theorem 1 are satisfied, from which the proof follows. ■

One limitation of Corollary 1 is that it requires $2n_{\mathbf{u}} \geq n_{\mathbf{x}}$. For many vehicle path planning problems, $2n_{\mathbf{u}} = n_{\mathbf{x}}$ since the state consists of the vehicle position and velocity, and the control acts on all elements of the vehicle velocity. We can extend Corollary 1 to the case of $2n_{\mathbf{u}} < n_{\mathbf{x}}$ for systems where there is additional structure in $\mathbf{f}(\cdot)$ and $\mathcal{F}$.

Condition 2: There exists a constant invertible matrix $T \in \Re^{(n_x \times n_x)}$ such that:

$$T^{-1}(\nabla_{\mathbf{x}} f)T = \begin{bmatrix}E\big(t, \mathbf{x}, \mathbf{u}, g_c(\mathbf{u})\big) & 0\end{bmatrix}, \quad (22)$$

where $E(\cdot) \in \Re^{n_x \times n_a}$ and $n_a < n_x$.

Theorem 2: Assume that Condition 2 holds and that $\mathcal{F}$ is defined as a plane such that $\mathcal{F} \triangleq \{\mathbf{x} : \mathbf{x} = Lv + \mathbf{a}_x\}$, where $L \in \Re^{n_x \times n_v}$. Let $\{\mathbf{u}^*, \mathbf{x}^*, t_f^*, \Gamma^*\}$ be the solution to Problem 2. Assume $l(t, \Gamma) \neq 0 \;\; \forall \Gamma \in [\rho_1, \rho_2], \; \forall t$. Define:

$$\tilde{M}(t) \triangleq \begin{bmatrix}M(t)\\ L^T\end{bmatrix} T^{-1}, \quad (23)$$

where $M(t)$ is as defined in (20). Then if $\tilde{M}(t)$ can be written:

$$\tilde{M}(t) = \begin{bmatrix}A & B\\ C & D\end{bmatrix} \qquad B = 0, \text{Null}(A) = 0, \text{Null}(D) = 0, \quad (24)$$

where $A \in \Re^{n_a \times n_a}$, then $\{\mathbf{u}^*, \mathbf{x}^*, t_f^*\}$ is the optimal solution to Problem 1.

Proof: As in Theorem 1 we show that $\mathbf{y}(t) = 0$ for a finite interval is not possible. Assume that there exists $t_1 < t_2$ such that $\mathbf{y}(t) = 0 \;\; \forall t \in [t_1, t_2]$. This implies that $\dot{\mathbf{y}}(t) = 0 \;\; \forall t \in [t_1, t_2]$. Define $\alpha = T\lambda = (\alpha_1, \alpha_2)$ where $\alpha_1 \in \Re^{n_a}$ and $\alpha_2 \in \Re^{n_x - n_a}$. Then $M(t)T^{-1}\alpha(t) = 0 \; \forall t \in [t_1, t_2]$. From the form of $\tilde{M}$ this means $A\alpha_1(t) = 0 \; \forall t \in [t_1, t_2]$ hence $\alpha_1(t) = 0 \; \forall t \in [t_1, t_2]$. From the costate dynamics:

$$\dot{\alpha}(t) = -T^{-1}(\nabla_{\mathbf{x}} f)T\alpha(t), \quad (25)$$

and since $\mathbf{f}(\cdot)$ satisfies Condition 2, we know that $\dot{\alpha}(t) = 0 \; \forall t \in [t_1, t_f^*]$, hence $\alpha(t) = \alpha(t_f^*) \; \forall t \in [t_1, t_f^*]$. The transversality condition[3] implies that $L^T T^{-1}\alpha(t_f^*) = 0$, hence $L^T T^{-1}\alpha(t) = 0 \; \forall t \in [t_1, t_f^*]$. Since $\alpha_1(t) = 0 \; \forall t \in [t_1, t_f^*]$, then $D\alpha_2(t) = 0 \; \forall t \in [t_1, t_f^*]$, which implies $\alpha_2(t) = 0 \; \forall t \in [t_1, t_f^*]$. Hence $\lambda(t) = 0 \; \forall t \in [t_1, t_f^*]$, which is a contradiction, and the proof proceeds as in Theorem 1. ■

Theorem 2 applies to vehicle-type problems where the dynamics of the states that are additional to velocity and position depend only on the control effort, and time, as we show in Corollary 2. An important practical example is the case where the vehicle has variable mass, and the rate of mass depletion depends only on the norm of the applied control effort, as we show in Section III.

Corollary 2: Let $f(\cdot)$ have the form:

$$\mathbf{x} = \begin{bmatrix}\mathbf{x}_3\\ \mathbf{x}_4\end{bmatrix} \qquad \mathbf{f}(t, \mathbf{x}, \mathbf{u}) = \begin{bmatrix}\mathbf{f}_3(t, \mathbf{x}, \mathbf{u})\\ \mathbf{f}_4(t, g_c(\mathbf{u}))\end{bmatrix}, \quad (26)$$

where $\mathbf{x}_3 \in \Re^{x_3}, \mathbf{x}_4 \in \Re^{x_4}$, and let L be defined such that $L^T = [L_1^T \; L_2^T]$ where $L_2 \in \Re^{n_{x_4} \times n_{x_4}}$. Define:

$$M_3 \triangleq \begin{bmatrix}(\nabla_{\mathbf{u}}\mathbf{f}_3)\\ \frac{d(\nabla_{\mathbf{u}}\mathbf{f}_3)}{dt} - (\nabla_{\mathbf{u}}\mathbf{f}_3)(\nabla_{\mathbf{x}}\mathbf{f}_3)\end{bmatrix}. \quad (27)$$

If $\text{Null}(M_3) = 0$, $\text{Null}(L_2) = 0$, and $l(t, \Gamma) \neq 0 \;\; \forall \Gamma \in [\rho_1, \rho_2], \; \forall t$ then the conclusions of Theorem 2 hold.

Proof: Choose $T = I$, then from the structure of $\mathbf{f}(\cdot)$ we have:

$$\tilde{M} = \begin{bmatrix} M_3 & 0 \\ L_1^T & L_2^T \end{bmatrix}, \tag{28}$$

where $\text{Null}(M_3) = 0$ and $\text{Null}(L_2^T) = 0$. Hence the conditions of Theorem 2 are satisfied. ∎

All of the convexification results presented in this paper rely on having an integral cost in Problem 1. The results, however, can be extended to the case of terminal cost using the two-step prioritized optimization strategy proposed in [5], [1]. First we solve a problem with relaxed control constraints and terminal cost, to determine the optimal terminal state. Then we solve a problem with a suitably-chosen integral cost with the terminal state constrained to be the optimal terminal state. From the convexification results presented in this paper, the second step ensures that the nonconvex control constraints are satisfied.

III. Practical Examples

In this section we use Theorem 1 to generate lossless convexifications for two practical examples, namely minimum-fuel soft landing with a general nonlinear gravity field and nonlinear aerodynamic drag, and path planning for a UAV with minimum and maximum velocity constraints. Both are problems of significant practical interest [12], [17], [2], [5], [15].

A. Minimum-fuel Landing with Nonlinear Gravity

The problem of minimum-fuel soft landing is stated as:

Problem 3 (Nonlinear-gravity soft landing):

$$\min_{\tau, t_f} J = \int_0^{t_f} ||\tau(t)|| dt \quad \text{subject to:} \tag{29}$$

$$\ddot{\mathbf{r}}(t) = \mathbf{g}(\mathbf{r}(t)) - C_D(\mathbf{r}(t))\|\dot{\mathbf{r}}(t)\|\dot{\mathbf{r}}(t) + \frac{\tau(t)}{m(t)} \tag{30}$$

$$\begin{aligned} &\dot{m}(t) = -\beta\|\tau(t)\| \\ &0 < \rho_1 \le ||\tau(t)|| \le \rho_2 \\ &\mathbf{r}(0) = \mathbf{r}_0, \quad \dot{\mathbf{r}}(0) = \dot{\mathbf{r}}_0, \\ &\mathbf{r}(t_f) = \mathbf{t}_p, \quad \dot{\mathbf{r}}(t_f) = \mathbf{t}_v, \end{aligned} \tag{31}$$

where $\mathbf{r} \in \Re^{n_r}$ denotes position, $\tau \in \Re^{n_r}$ denotes thrust[1], $m \in \Re$ denotes mass, and $\mathbf{t}_p \in \Re^{n_r}$ and $\mathbf{t}_v \in \Re^{n_r}$ denote the position and velocity targets, respectively. C_D is a constant related to the drag coefficient of the spacecraft and the atmospheric density, β relates to the specific impulse of the thrusters, and $\mathbf{g}(\cdot)$ is the (possibly nonlinear) acceleration due to gravity. Therefore, letting $\mathbf{x} \triangleq (\dot{\mathbf{r}}, \mathbf{r}, m)$ and $\mathbf{u} \triangleq \tau$, we can express this problem as Problem 1 with:

$$l(t, v) = v, \; g_c(\mathbf{u}) = \|\mathbf{u}\|, \mathbf{x}_0 = (\dot{\mathbf{r}}_0, \mathbf{r}_0, m) \tag{32}$$

$$\mathcal{F} = \{\mathbf{x} : \mathbf{r} = \mathbf{t}_p, \dot{\mathbf{r}} = \mathbf{t}_v\} \tag{33}$$

$$\mathbf{f}(t, \mathbf{x}, \mathbf{u}) = \begin{bmatrix} \mathbf{f}_5(t, \mathbf{x}, \mathbf{u}) \\ \mathbf{f}_6(t, \mathbf{x}) \\ \mathbf{f}_7(t, g_c(\mathbf{u}(t))) \end{bmatrix} = \begin{bmatrix} \mathbf{g}(\mathbf{r}) - C_D\|\dot{\mathbf{r}}\|\dot{\mathbf{r}} + \tau/m \\ \dot{\mathbf{r}} \\ -\beta||\tau|| \end{bmatrix}. \tag{34}$$

The function $\mathbf{f}(\cdot)$ falls into the form of Corollary 2, with $\mathbf{f}_4 = \mathbf{f}_7$ and $\mathbf{f}_3 = (\mathbf{f}_5, \mathbf{f}_6)$. We have:

$$(\nabla_{\mathbf{u}} \mathbf{f}_5) = I \qquad (\nabla_{\dot{\mathbf{r}}} \mathbf{f}_6) = I, \tag{35}$$

hence from Corollary 1 we know $\text{Null}(M_3) = 0$. Now, $l(t, \Gamma) \neq 0 \;\; \forall \Gamma \in [\rho_1, \rho_2], \; \forall t$. Since the final state is all constrained except for $m(t_f)$, we can write $\mathcal{F} = \{\mathbf{x} | \mathbf{x} = Lv + \mathbf{a}_x\}$ with $v \in \Re$ and $L_1 = 0_{6\times1}$ and $L_2 = 1$. Hence the conditions of Corollary 2 are satisfied and we can obtain the optimal solution of this problem by solving its relaxed version given by Problem 2.

The special case of constant gravity and no aerodynamic drag, where $\mathbf{g}(\mathbf{r}(t)) \triangleq \mathbf{g}$ and $C_D = 0$, was handled by [2], which is now generalized to the nonlinear gravity case with aerodynamic drag by Theorem 2. In Section IV we give simulation results for the general nonlinear gravity case. For extensive results on the special case of constant gravity, we refer the reader to [2].

B. Velocity-controlled Aircraft

In this section we consider the problem of controlling an aircraft subject to maximum and minimum velocity constraints, and subject to aerodynamic drag proportional to the square of velocity. The aircraft is modeled as having an inner-loop proportional controller that regulates the velocity to a desired reference value[15].

Problem 4 (UAV with velocity constraints):

$$\min_{\mathbf{v}_d, t_f} J = \int_0^{t_f} l\big(||\mathbf{v}_d(t)||\big) dt \quad \text{subject to:} \tag{36}$$

$$\begin{aligned} &\ddot{\mathbf{r}}(t) = \kappa\big(\mathbf{v}_d(t) - \dot{\mathbf{r}}(t)\big) - C_D\dot{\mathbf{r}}(t)\|\dot{\mathbf{r}}(t)\| \\ &0 < \rho_1 \le ||\mathbf{v}_d(t)|| \le \rho_2 \\ &\mathbf{r}(0) = \mathbf{r}_0 \quad \dot{\mathbf{r}}(0) = \dot{\mathbf{r}}_0 \\ &\mathbf{r}(t_f) = \mathbf{r}_f \quad \dot{\mathbf{r}}(t_f) = \dot{\mathbf{r}}_f, \end{aligned}$$

where $\mathbf{r}$ denotes position, $\mathbf{v}_d$ denotes reference velocity, κ denotes the gain of the inner-loop controller, $\mathbf{r}_f$ denotes desired final position and $\dot{\mathbf{r}}_f$ denotes desired final velocity. The function $l(\cdot)$ is a cost function that may be nonlinear and nonconvex, as long as $l(v) \neq 0$ for $\rho_1 \le v \le \rho_2$. This problem can be written as Problem 1 with $\mathbf{x} = (\dot{\mathbf{r}}, \mathbf{r})$, $\mathbf{u} = \mathbf{v}_d$, and:

$$\begin{aligned} &\mathbf{f}(t, \mathbf{x}, \mathbf{u}) = \begin{bmatrix} \mathbf{f}_1(t, \mathbf{x}, \mathbf{u}) \\ \mathbf{f}_2(t, \mathbf{x}) \end{bmatrix} = \begin{bmatrix} -\kappa\dot{\mathbf{r}} - C_D\dot{\mathbf{r}}\|\dot{\mathbf{r}}\| + \kappa\mathbf{v}_d \\ \dot{\mathbf{r}} \end{bmatrix} \\ &g_c(\mathbf{u}) = \|\mathbf{v}_d\| \qquad \mathbf{x}_0 = (\mathbf{r}_0, \dot{\mathbf{r}}_0), \\ &\mathcal{F} = \{\mathbf{x} : \mathbf{x}_1 = \dot{\mathbf{r}}_f, \mathbf{x}_2 = \mathbf{r}_f\}. \end{aligned}$$

[1]Note that thrust here is not a true force, but an effective force, which is proportional to the rate at which mass is expelled by the thrusters. We refer the reader to standard texts on the rocket equation, such as [6].

Now we can apply Corollary 1 and solve Problem 2 to obtain optimal solutions of this problem.

IV. Simulation Results

Here we present simulation results for a two-dimensional soft landing problem with nonlinear gravity, as defined in Problem 3 with $\mathbf{r} \in \Re^2$. Figure 3 shows the piecewise linear gravity model used in this section. For this example we set $\alpha = C_D = 0$. Figures 4 and 5 show the solution to the relaxed version of Problem 3 given by Problem 2 with the problem parameters are given as in (32) through (34). Here the nonlinear gravitational field $\mathbf{g}(\mathbf{r})$ is approximated by a piecewise gravitational acceleration $\hat{\mathbf{g}}(\mathbf{r})$, which is as follows:

$$\hat{\mathbf{g}}(\mathbf{r}) \triangleq \mathbf{A}_i \mathbf{r} + \mathbf{b}_i \quad \forall \mathbf{r} \in \mathcal{P}_i, \tag{37}$$

where $\mathcal{P}_i$ is a convex polytope defined by:

$$\mathcal{P}_i \triangleq \{\mathbf{r} | P_i \mathbf{r} \leq \mathbf{p}_i\}. \tag{38}$$

The feasible space of positions is partitioned into n_z polytopes. In the numerical example in this section we assume that $\mathbf{g}(\mathbf{r})$ depends only on altitude, and partition the altitude into intervals. We then define $\mathbf{A}_i$ and b_i so that the piecewise linear section for interval $\mathcal{P}_i$ is tangent to $\hat{\mathbf{g}}(\mathbf{r})$ at the midpoint of $\mathcal{P}_i$. An example is given in Figure 3. The 2-norm constraint $\|\tau(t)\| \leq \Gamma(t)$ is approximated by using a 32-sided polygon at each discretization time instance, which is shown in Figure 1, as follows:

$$\mathbf{a}_j^T \tau_k \leq \Gamma_k \quad j = 1, \ldots, n_p, \tag{39}$$

where n_p is the number of facets used to approximate the 2-norm constraint, and $\mathbf{a}_i$ is a vector normal to the facet, scaled so that the polytope defined by (39) is an inner approximation of the hypersphere defined by $\|\tau(t)\| \leq \Gamma(t)$. An example of such an approximation is given in Figures 1 and 2.

Given the above approximations of gravity and control constraints, and the fact that the cost is linear in the slack variable Γ, the relaxed optimal control problem, Problem 2 with (32), can be discretized to obtain a Mixed Integer Linear Program[10] for each final time t_f. Details are given in the Appendix. We use $N = 15$ discretization time steps[2]. The resulting MILP can then be solved to global optimality using highly optimized commercial solvers[11]. Since t_f is a scalar solution variable, we can find the global optimum solution of the problem by performing a line search on t_f, solving a MILP at each cost computation during the line search. We use the Golden Search method [4] to do so.

The simulation results in Figure 5 show that the nonconvex control magnitude constraints are satisfied as predicted by Theorem 1. For this example we used $\rho_1 = 2\text{m/s}^2$, $\rho_2 = 10\text{m/s}^2$, $\mathbf{r}_0 = [2, 8] \times 10^4\text{m}$, $\dot{\mathbf{r}}_0 = \mathbf{t}_p = \mathbf{t}_v = 0$. The optimal solution had $t_f^* = 490\text{s}$.

[2]Our empirical experience has shown that increasing the number of discretization steps above N=15 has only a very minor impact on the resulting solution.

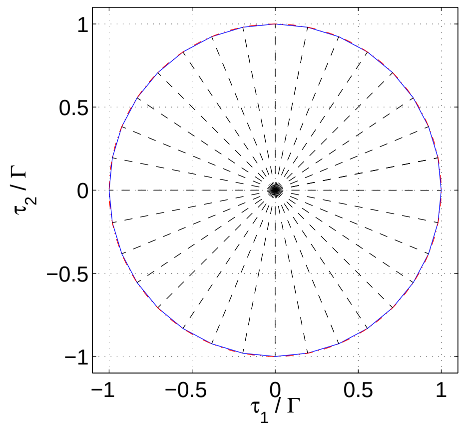

Fig. 1. Polygonal approximation of thrust 2-norm constraint.

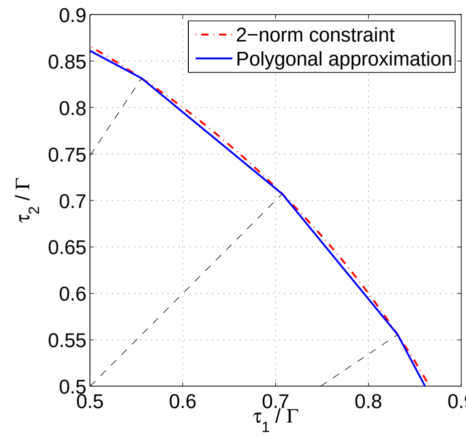

Fig. 2. Detail of polygonal approximation of thrust 2-norm constraint.

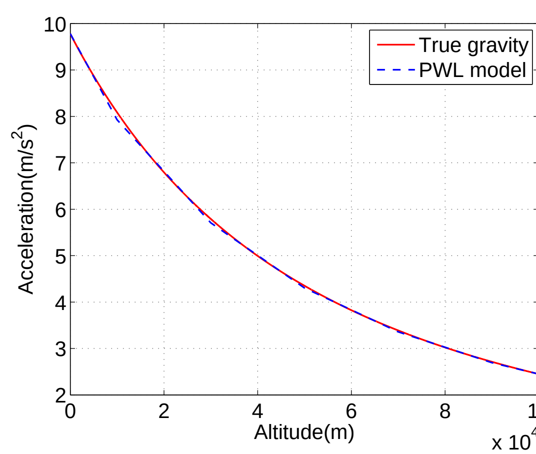

Fig. 3. Nonlinear gravity model and piecewise linear (PWL) approximation.

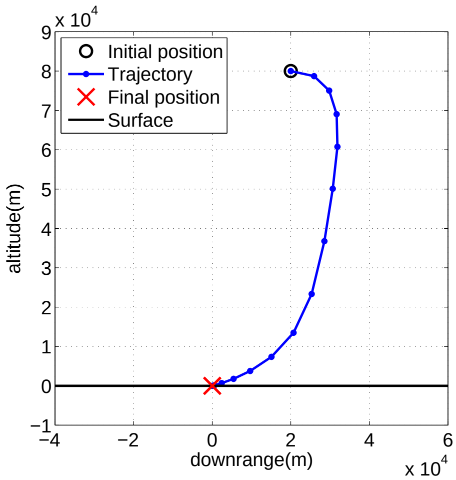

Fig. 4. Optimal trajectory for nonlinear soft landing problem.

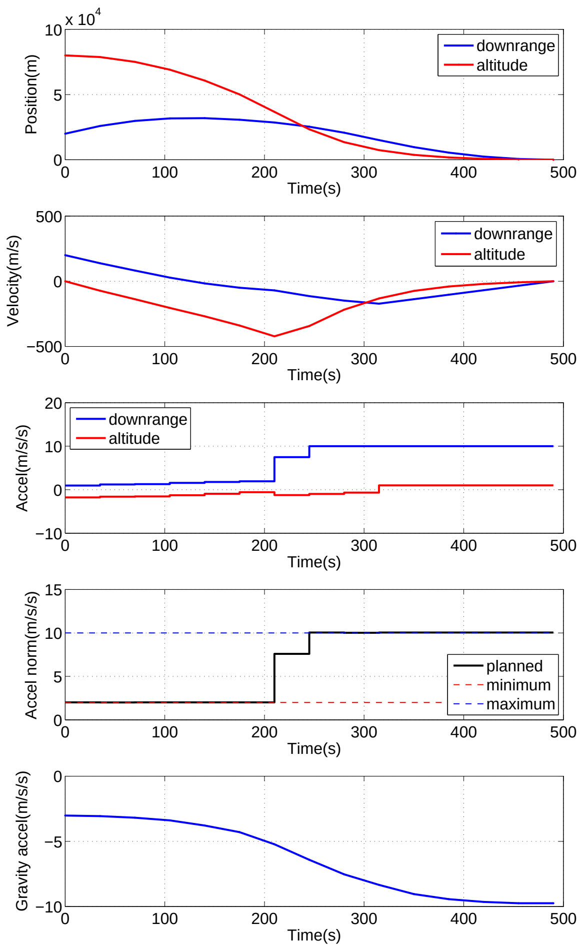

Fig. 5. Optimal profiles for nonlinear soft landing problem. Note the nonconstant, nonlinear acceleration due to gravity. The nonconvex control acceleration constraints are satisfied, as predicted by Theorem 1.

V. Discussion

In this section we make some remarks on two alternative approaches to handling the nonconvex control constraints in Problem 1. The first approach is to approximate the nonconvex constraint $\rho_1 \leq g_c(\mathbf{u}(t))$ as a polytopic stay-out region, and use binary variables to encode the resulting problem as a MILP. This was proposed by [14] for a UAV path-planning problem. Although our convexification approach also results in a MILP, the number of binary variables is significantly reduced by removing the nonconvexity in the control constraints. Since a MILP is worst-case exponential in the number of binary variables, this yields a large improvement in the problem complexity.

The second approach is to perform a change of variables to render the control constraints convex. For lower and upper bounds on the 2-norm, as in our practical examples, this can be achieved by a conversion to polar coordinates. The major disadvantage of this approach, however, is that it simply shifts the nonconvexity from the control constraints to the dynamics. In the case of polar coordinates, this leads to trigonometric functions in the dynamics. For many problems, in cartesian coordinates, the system dynamics are linear with some structured nonlinearity, which can be approximated as being piecewise linear without an explosion in the number of binary variables in the resulting MILP. A conversion to polar coordinates requires every n_x-dimensional equality constraint in the dynamics to be modeled as being piecewise linear. This will typically lead to many more binary variables than the convexification approach proposed in this paper.

VI. Conclusion

This paper provided a lossless convexification of a class of optimal control problems that have continuous-time nonlinear dynamics and nonconvex control constraints. We prove that the optimal solution to the relaxed problem is the globally optimal solution to the original nonconvex problem. We demonstrated the approach in simulation with a planetary soft landing problem.

Appendix

In this section we describe a method for approximating the relaxation of the infinite-dimensional soft landing problem (Problem 3) as a finite-dimensional optimization problem that can be solved to global optimality using Mixed Integer Linear Programming (MILP). We introduce the following approximations:

1) In order to reduce the infinite-dimensional to a finite-dimensional one, we perform a standard discretization in time assuming a zero-order hold (ZOH) on the control inputs $\mathbf{u}$.
2) We approximate the smooth nonlinear function $\mathbf{g}(\mathbf{r}(t))$ as a piecewise linear function, as in (37) through (38).
3) We approximate the norm bounds using convex polytopic constraints as in (39).

We then show that, for fixed Δt, the resulting problem is a MILP. This means that, by performing a line search over Δt, as proposed in [2], we can find the globally optimal solution.

For simplicity of exposition, we assume that mass is constant, even though this nonlinearity could be handled through piecewise linearization in a similar manner to the gravity. An alternative method for dealing with time-varying mass, which moves the nonlinearity from the dynamics into the constraints, was previously proposed by [2].

A. Time discretization

To perform the time-discretization we define a fixed number of time steps N, and a time step Δt such that $t_f = N\Delta t$. Define a discrete-time set of variables that approximate the continuous time variables: $\mathbf{r}_k \triangleq \mathbf{r}(k\Delta t),\ \dot{\mathbf{r}}_k \triangleq \dot{\mathbf{r}}(k\Delta t)$. We restrict the class of control input sequences $\tau(t)$ and $\Gamma(t)$ to be of a zero-order hold type, such that:

$$\begin{aligned}\tau(t) &= \tau_k \quad \forall t \in [k\Delta t, (k+1)\Delta t)\\ \Gamma(t) &= \Gamma_k \quad \forall t \in [k\Delta t, (k+1)\Delta t).\end{aligned} \tag{40}$$

By approximating the gravity value $\mathbf{g}(\mathbf{r}(t))$ as constant for all $t \in [k\Delta t, (k+1)\Delta t]$, the dynamics of the spacecraft (30) can be written in discrete-time as:

$$\begin{aligned}\mathbf{r}_{k+1} &= \mathbf{r}_k + \dot{\mathbf{r}}_k\Delta t + \frac{1}{2}\Delta t^2\Big(\frac{\tau_k}{m_{wet}} + \mathbf{g}(\mathbf{r}_k)\Big)\\ \dot{\mathbf{r}}_{k+1} &= \dot{\mathbf{r}} + \Delta t\Big(\frac{\tau_k}{m_{wet}} + \mathbf{g}(\mathbf{r}_k)\Big).\end{aligned} \tag{41}$$

Note that these dynamics are still nonlinear due to the nonlinear dependence of $\mathbf{g}(\mathbf{r}_k)$ on $\mathbf{r}_k$. The cost function is:

$$J = \Delta t \sum_{i=0}^{N-1} \Gamma_k. \tag{42}$$

B. MILP formulation

The relaxation of Problem 3 can now be approximated as follows:

Problem 5 (MILP approximation of landing problem):

$$\min_{\Delta t, \tau_i, \Gamma_i, z_{ik}} J = \Delta t \sum_{i=0}^{N-1} \Gamma_i \tag{43}$$

subject to, for all $i = 1, \dots, n_z, k = 1, \dots, N-1$:

$$P_i \mathbf{r}_k \le \mathbf{p}_i + M z_{ik} \tag{44}$$

$$\begin{aligned}\mathbf{r}_{k+1} &\le \mathbf{r}_k + \dot{\mathbf{r}}_k\Delta t + \frac{1}{2}\Delta t^2\Big(\frac{\tau_k}{m_{wet}} + A_i\mathbf{r}_k + \mathbf{b}_i\Big) + M z_{ik}\\ \mathbf{r}_{k+1} &\ge \mathbf{r}_k + \dot{\mathbf{r}}_k\Delta t + \frac{1}{2}\Delta t^2\Big(\frac{\tau_k}{m_{wet}} + A_i\mathbf{r}_k + \mathbf{b}_i\Big) - M z_{ik}\end{aligned} \tag{45}$$

$$\begin{aligned}\dot{\mathbf{r}}_{k+1} &\le \dot{\mathbf{r}} + \Delta t\Big(\frac{\tau_k}{m_{wet}} + A_i\mathbf{r}_k + \mathbf{b}_i\Big) + M z_{ik}\\ \dot{\mathbf{r}}_{k+1} &\le \dot{\mathbf{r}} + \Delta t\Big(\frac{\tau_k}{m_{wet}} + A_i\mathbf{r}_k + \mathbf{b}_i\Big) - M z_{ik}\end{aligned} \tag{46}$$

$$z_{ik} \in \{0, 1\}, \tag{47}$$

where M is a large positive integer, subject to:

$$\sum_{i=1}^{n_z} z_{ik} \le n_z - 1 \quad k = 1, \dots, N-1 \tag{48}$$

$$\mathbf{a}_j^T \tau_k \le \Gamma_k \quad j = 1, \dots, n_p, k = 1, \dots, N-1 \tag{49}$$

$$0 < \rho_1 \le \Gamma_k \le \rho_2 \quad k = 1, \dots, N-1. \tag{50}$$

and subject to $\mathbf{r}_N = \mathbf{r}_f, \dot{\mathbf{r}}_N = \dot{\mathbf{r}}_f$.

In Problem 5, the binary variables z_{ik} are used to indicate which polytope $\mathcal{P}_i$ the position $\mathbf{r}_k$ lies in. The constraint (48) ensures that at least one of the z_{ik} is zero at each time step. For whichever $\mathcal{P}_i$ has $z_{ik} = 0$, the constraints (45) and (46) use 'big-M' formulation[15] to ensure that the dynamic equality constraints are satisfied, while (44) ensures that $\mathbf{r}_k$ lies in $\mathcal{P}_i$. For fixed Δt, since all of the constraints are linear, the cost function is linear, and we have integer variables, Problem 5 is a Mixed Integer Linear Program. This means it can be solved to global optimality using highly optimized commercial solvers[11]. Since Δt is a scalar, we can find the global optimum to Problem 5 by performing a line search on Δt, solving a MILP at each iteration. We use the Golden Search method[4] to do so.

In summary, the relaxed soft landing problem with nonlinear gravity can be approximated using the approach described in this section, and solved to global optimality using existing techniques.

References

[1] B. Açıkmeşe and L. Blackmore. Lossless convexification of a class of optimal control problems with non-convex control constraints. *Automatica*, 47(2), 2011.

[2] B. Açıkmeşe and S. R. Ploen. Convex programming approach to powered descent guidance for Mars landing. *AIAA Journal of Guidance, Control and Dynamics*, 30(5):1353–1366, 2007.

[3] L. D. Berkovitz. *Optimal Control Theory*. Springer-Verlag, 1975.

[4] D. P. Bertsekas. *Nonlinear Programming, second edition*. Athena Scientific, 2000.

[5] L. Blackmore, B. Açıkmeşe, and D. P Scharf. Minimum landing error powered descent guidance for Mars landing using convex optimization. *AIAA Journal of Guidance, Control and Dynamics*, 33(4):1161–1171, 2010.

[6] H. Curtis. *Orbital Mechanics for Engineering Students, 2nd Edition*. Elsevier, 2010.

[7] H. D'Angelo. *Linear Time-Varying Systems: Analysis and Synthesis*. Allyn and Bacon, 1970.

[8] F. Fahroo and I. M. Ross. Direct trajectory optimization by a Chebyshev pseudospectral method. *Journal of Guidance, Control, and Dynamics*, 25(1):160–166, 2002.

[9] W. H. Flemming and R. W. Rishel. *Deterministic and Stochastic Optimal Control*. Springer-Verlag, 1975.

[10] C. A. Floudas. *Nonlinear and Mixed-Integer Programming - Fundamentals and Applications*. Oxford University Press, 1995.

[11] ILOG. ILOG CPLEX user's guide, 1999.

[12] A. R. Klumpp. Apollo lunar descent guidance. *Automatica*, 10:133–146, 1974.

[13] J. S. Meditch. On the problem of optimal thrust programming for a lunar soft landing. *IEEE Transactions on Automatic Control*, AC-9(4):477–484, 1964.

[14] T. Schouwenaars. *Safe Trajectory Planning of Autonomous Vehicles*. PhD thesis, Massachusetts Institute of Technology, 2006.

[15] T. Schouwenaars, B. De Moor, E. Feron, and J. How. Mixed integer programming for multi-vehicle path planning. In *Proc. European Control Conference*, 2001.

[16] R. Sostaric and J. Rea. Powered descent guidance methods for the moon and mars. *AIAA Guidance, Navigation, and Control Conference, San Francisco, CA*, 2005.

[17] B. A. Steinfeldt, M. J. Grant, D. A. Matz, R. D. Braun, and G. H. Barton. Guidance, navigation and control system performance trades for mars pinpoint landing. *Journal of Spacecraft and Rockets*, 47(1):188–198, 2010.

[18] U. Topcu, J. Casoliva, and K.D. Mease. Fuel efficient powered descent guidance for mars landing. *AIAA Guidance, Navigation, and Control Conference, San Francisco, CA*, 2005.